

Impacts of the Negative-exponential and the K-distribution modeled FSO turbulent links on the theoretical and simulated performance of the distributed diffusion networks

S. Tannaz, C. Ghobadi, J. Nourinia

Department of Electrical and Computer Engineering, Urmia University, Urmia, Iran
s.tannaz@urmia.ac.ir, ghobadi.changiz1@gmail.com, nourinia.javad1@gmail.com

Corresponding author: s.tannaz@urmia.ac.ir

Abstract- Merging the adaptive networks with the free space optical (FSO) communication technology is a very interesting field of research because by adding the benefits of this technology, the adaptive networks become more efficient, cheap and secure. This is due to the fact that FSO communication uses unregistered visible light bandwidth instead of the overused radio spectrum. However, in spite of all the benefits of FSO communication, this technology suffers from optical noise and turbulence. In this paper, we investigate the exact effect of the negative exponential and k-distribution modeled very strong turbulence conditions on the performance of diffusion adaptive networks. The simulation and theoretical results based on the steady state Mean square deviation (MSD) and Excess mean square Error (EMSE) values show the deteriorating effects of these link models on diffusion networks. The FSO communication technology, while very profitable and applicable, is not always a suitable means of implementing wireless networks. For this reason, we suggested the channel estimation for these conditions.

Index Terms- Log-normal distribution, Turbulence, Negative-exponential, K-distribution, FSO, distributed diffusion networks,

I. INTRODUCTION

The function of the adaptive network is to estimate an unknown vector (\mathbf{w}^o). This estimation can be taking place in an optical FSO environment and the effects of this environment must be analyzed on the estimation performance of the network. The performance is then depicted in the form of steady-state error values that are MSD and EMSE metrics. The FSO communication systems can be introduced with their various advantages. They have wide unregistered frequency bandwidths, they do not need the digging as for optical fibers, and their equipment is cheaper, less heavy and more precise

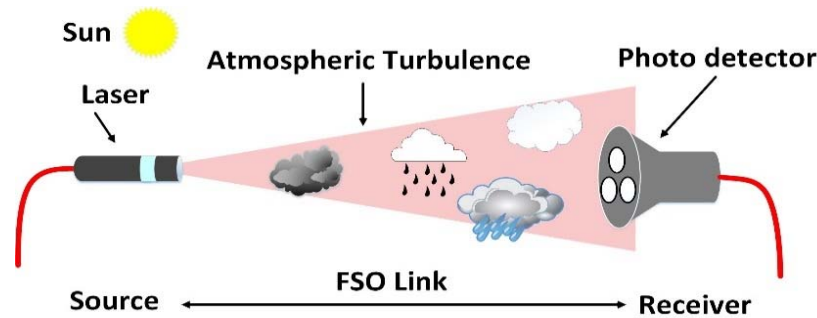


Fig. 1. The FSO links with turbulence.

than the Radio Frequency (RF) systems [1]. The FSO channels have characteristics that are special to them. They have a famous barrier namely the optical turbulence. These turbulences are caused by environmental effects such as rain, fog, etc. Fig. 1 represents some of the problems of the FSO link and as they are random, they can be modeled with statistical distributions.

In many references and experimental studies, the goal has been to model the statistical behavior of this turbulence [1, 3]. Also, many papers such as [2] have been published recently describing the effects of these turbulence models on various communication systems that are implemented with the wireless optical technology. This is an important topic of research because, if we want to migrate a communication system from the RF to the FSO technology, first we must be sure that this change is worthwhile and the system will not face with unsolvable problems. One of these systems that can be migrated to the FSO platform is the diffusion adaptive network. However, as the main purpose of using adaptive networks is the monitoring and estimation of environmental parameters, precision is very important in their tasks. When the FSO channel is not highly turbulent, we can expect that the diffusion network that is implemented with this technology work properly. But for the cases that the turbulence is very strong, the same thing cannot be said. Therefore, the precise evaluation of the FSO channel effects on the adaptive diffusion networks can be an important way of the decision to implement them with FSO technology or not.

The statistical models for describing the FSO link models focus on modeling different levels of optical turbulence [3]. For this reason, various distributions are proposed like the log-normal distribution [1, 3 and 15] for the weak to moderate turbulence, gamma-gamma distribution [7,12] to model weak to strong turbulence and the negative exponential [3, 6] and K-distribution [4, 10] for modeling strong turbulence. In this paper, we especially focus on the strong turbulence of FSO links in order to emphasize the importance of the channel estimation for the adaptive networks that are implemented in these conditions [16, 17].

The diffusion adaptive networks are the best tools for distributed data processing in many applications. However, in monitoring and wireless applications the diffusion network must work in non-ideal conditions and therefore, the link noise and coefficients must be taken into consideration.

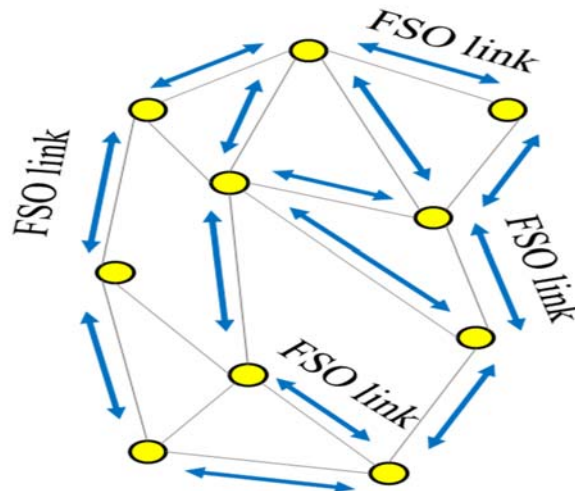


Fig. 2. The Diffusion network implemented with the FSO links.

The performance of diffusion networks in noisy links has been considered in [13]. Also, their performance in fading conditions has been studied in [14] where the link coefficients follow the Rayleigh distribution. In [15], the performance of diffusion adaptive networks has been considered in FSO links. Fig. 2 shows a diffusion network implemented with FSO communication technology.

In [15, 20] only the Log-normal and Gamma-Gamma distributions were considered for modeling FSO link turbulences. In this paper, however, we consider the negative exponential and K-distribution models for modeling FSO link coefficients. Finally, in [20], the effects of Radio channel coefficients on the performance of the diffusion adaptive networks has been considered and in this papers we used the theoretical findings of that paper and applied them to the FSO link conditions.

The first contribution of this paper is that in this research, for the first time, we present a detailed explanation and framework for generating the FSO link coefficients in strong turbulence conditions, their parameters and PDFs. The second contribution of this paper is investigating the performance of diffusion adaptive networks with FSO links in the presence of strong turbulence with negative exponential and K-distribution.

The rest of this research is organized as follows: in part II, the formulation of diffusion adaptation in the FSO links is considered. In part III, we considered the FSO channel modeling and the detailed parameters and PDFs that are attributed to the strong turbulence model distributions. Part IV. Belong to the simulation results and part V contains the concluding remarks and the future scope.

Notation: throughout this paper, we adopted the small-bold faced letters for vectors, capital bold-faced letters for matrices and regular font letters for scalar variables. Also, operator $\mathbb{E}[\cdot]$ is used for presenting the statistical expectation.

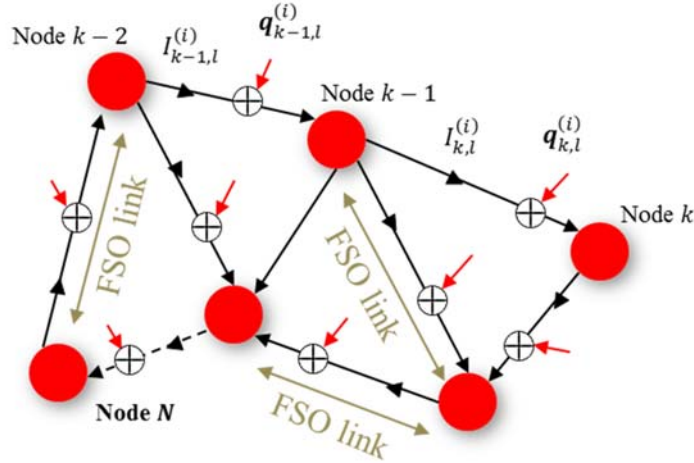


Fig. 3. The Diffusion network with the FSO links impairments.

II. PROBLEM STATEMENT

In order to investigate the performance of adaptive diffusion networks with FSO link conditions, we design a network containing N nodes that pursue the weight vector \mathbf{w}^o with the size of $(M \times 1)$. Each node in this network has access to $\mathbf{u}_{k,i}$ and $d_k(i)$ variables at each iteration that is the input regressor vector and the scalar desired output respectively. The linear relation between these two variables at each stage is as follows:

$$d_k(i) = \mathbf{u}_{k,i} \mathbf{w}^o + v_k(i) \quad (1)$$

The network is asked to converge to the \mathbf{w}^o vector iteratively with the presence of measurement noise showed as $v_k(i)$. The diffusion adaptation can be implemented with two strategies: the adapt then combine (ATC) and the combine then adapt (CTA). These two algorithms in FSO links work differently from the ideal conditions and therefore, their formulation must contain link coefficients and link noise. Fig. 3 shows a diffusion adaptive network with non-ideal FSO links. In Fig. 3, $I_{k,l}^{(i)}$ shows the FSO link coefficients (or Irradiance coefficients as in [3]) between node k and l . Also, $\mathbf{q}_{k,l}^{(i)}$ is used for showing the link noise vector between the same nodes that is additive white Gaussian. In the FSO link conditions the $\mathbf{q}_{k,l}^{(i)}$ variables, usually follow the normal distribution and the $I_{k,l}^{(i)}$ variables follow the optical turbulence models that are described in section III. Here we describe the two diffusion strategies in FSO link conditions:

A. The Diffusion Combine Then Adapt (CTA) Method in Turbulent Link Conditions

The CTA strategy starts with combining the received weight estimations from neighboring nodes. However, in turbulent FSO link conditions and at iteration i , these received estimations are multiplied

with FSO link coefficients $I_{k,l}^{(i)}$ and added by channel noise vector ($\mathbf{q}_{k,l}^{(i)}$) between node l and k . The result at node k is $\mathbf{t}_{k,l}^{(i)}$ that is received from node l :

$$\mathbf{t}_{k,l}^{(i)} = I_{k,l}^{(i)} \boldsymbol{\psi}_k^{(i)} + \mathbf{q}_{k,l}^{(i)}, \quad l \in \mathcal{N}_k \quad (2)$$

In this relation, \mathcal{N}_k represents the number of neighboring nodes of node k . It is important to mention that we choose $\mathcal{N}_k = 7$ in our simulations. The combination equation for this CTA becomes [15]:

$$\boldsymbol{\phi}_k^{(i-1)} = \sum_{l \in \mathcal{N}_k} a_{k,l} \mathbf{t}_{k,l}^{(i-1)} \quad (3)$$

After collecting the local estimations of all neighboring nodes, the node k combines them with $a_{k,l}$ coefficients that are produced in a uniform manner as [15]:

$$a_{l,k} = \begin{cases} \frac{1}{n_k}, & l \in \mathcal{N}_k \\ 0, & otherwise \end{cases} \quad (4)$$

At the final stage of the CTA strategy, the node k updates its estimation using its received data and the Least mean square (LMS) algorithm with the step size of μ_k :

$$\boldsymbol{\psi}_k^{(i)} = \boldsymbol{\phi}_k^{(i-1)} + \mu_k \mathbf{u}_{k,i}^* (d_k(i) - \mathbf{u}_{k,i} \boldsymbol{\phi}_k^{(i-1)}) \quad (5)$$

B. The Diffusion Adapt Then Combine (ATC) Method in Turbulent Link Condition

In this mode of cooperation we first update the local estimation of node k using the received data:

$$\boldsymbol{\phi}_k^{(i)} = \boldsymbol{\psi}_k^{(i-1)} + \mu_k \mathbf{u}_{k,i}^* (d_k(i) - \mathbf{u}_{k,i} \boldsymbol{\psi}_k^{(i-1)}) \quad (6)$$

Next, we collect the local estimations of the neighboring nodes that are received through the FSO links and we show them as [15]:

$$\mathbf{r}_{k,l}^{(i)} = I_{k,l}^{(i)} \boldsymbol{\phi}_k^{(i)} + \mathbf{q}_{k,l}^{(i)}, \quad l \in \mathcal{N}_k \quad (7)$$

Finally, we combine them with the uniform coefficients:

$$\boldsymbol{\psi}_k^{(i)} = \sum_{l \in \mathcal{N}_k} a_{k,l} \mathbf{r}_{k,l}^{(i)} \quad (8)$$

III. Results FSO link descriptions with strong turbulence

Here, we give the detailed descriptions of the used FSO link models that are ascribed for the irradiance $I_{k,l}^{(i)}$ coefficients. We focus on models that describe especially the strong turbulence conditions:

A. K-distribution Model

The K-distribution can be achieved as a multiplication of one Exponential distribution and one Gamma distribution [4]. The PDF of this distribution is, therefore:

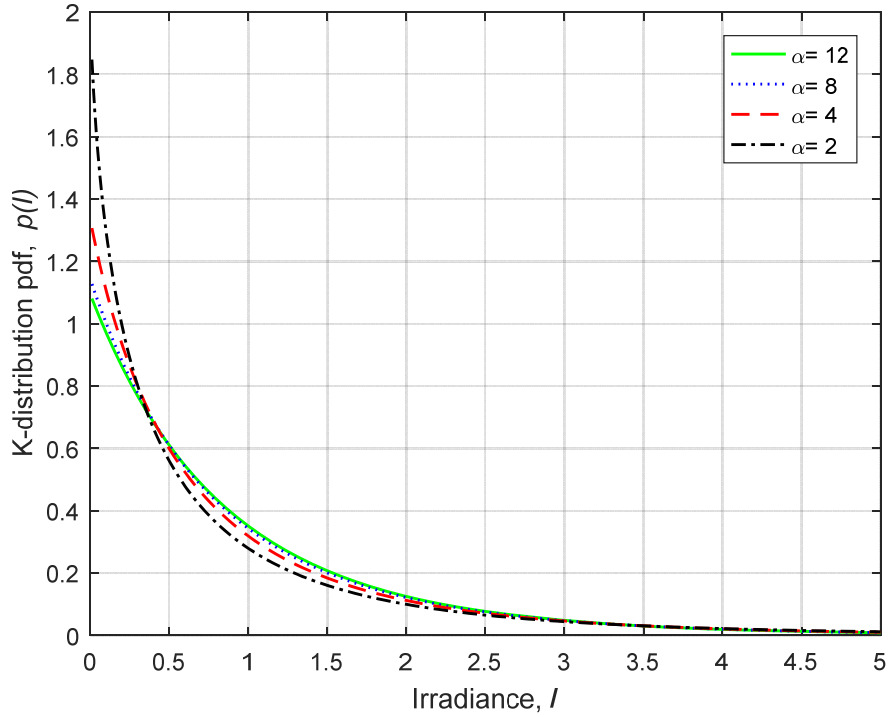


Fig. 4. The K-distribution PDFs with respect to various α values.

Table I. The statistical values of the K-distribution link.

For the K-distribution model		
α	$E[I] = m_k$	$E[I^2] = s_k$
2	1	1.9735
4	1	1.4906
8	1	1.2678
12	1	1.1556

$$f_I(I) = \frac{2\alpha^{\frac{(\alpha-1)}{2}}}{\Gamma(\alpha)} I^{\frac{(\alpha-1)}{2}} K_{\alpha-1}(2\sqrt{\alpha I}), I > 0 \tag{9}$$

Here $\Gamma(\cdot)$ Shows the Gamma function and $K_n(\cdot)$ is used for showing the n th order modified Bessel function of the second kind. Also, α is a parameter depending on the effective number of discrete scatters. The PDFs are given in Fig. 4. The statistical values for this distribution are given in Table I.

B. Negative-Exponential Model

The negative exponential distribution is another model that is widely accepted for the modeling of strong turbulence conditions [3, 6]. The PDF of this distribution is given as:

$$P(I) = \frac{1}{I_0} \exp\left(-\frac{I}{I_0}\right), I_0 > 0 \tag{10}$$

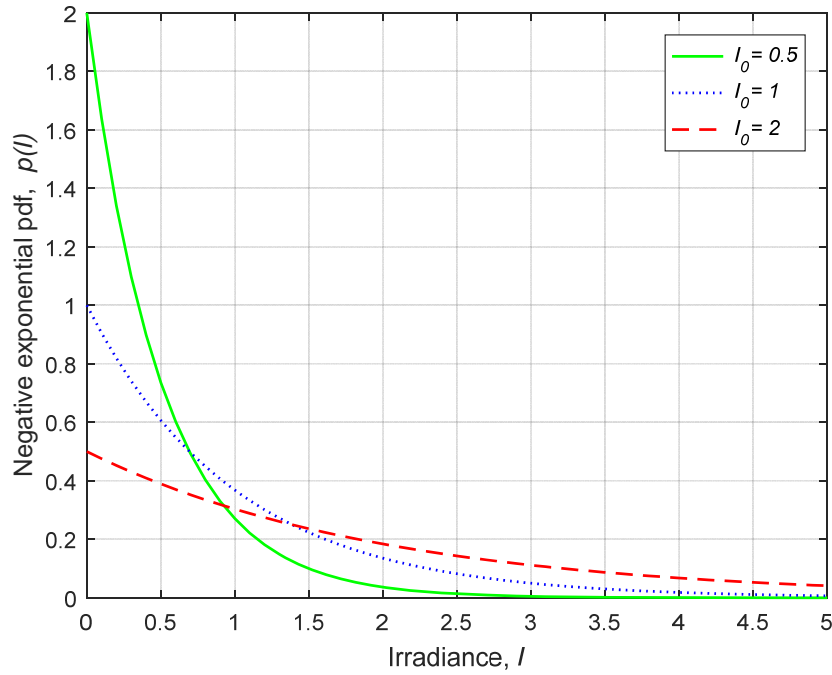


Fig. 5. The Negative Exponential PDFs with respect to $E[I] = I_0$ values.

Table II. The statistical values of the Negative exponential link.

For the Negative exponential model		
I_0	$E[I] = m_k$	$E[I^2] = s_k$
0.5	0.5	0.25
1	1	1
2	2	4

where $E[I] = I_0$ is the mean of receiver optical irradiance. The negative exponential PDF is shown in Fig. 5 for various values of I_0 . And the statistical values for the Negative exponential distribution are given in Table II.

III. THEORETICAL ANALYSIS

In order to evaluate the performance of the diffusion LMS algorithm with the CTA strategy in FSO channel conditions, we define the following criteria:

$$MSD_k \triangleq \lim_{i \rightarrow \infty} \mathbb{E} \left[\|\tilde{\boldsymbol{\psi}}_{k-1}^{(i)}\|_I^2 \right] \tag{11}$$

$$EMSE_k \triangleq \lim_{i \rightarrow \infty} \mathbb{E} \left[\|\tilde{\boldsymbol{\psi}}_{k-1}^{(i)}\|_{\mathbf{R}_{u,k}}^2 \right] \tag{12}$$

where the weighted norm for the exemplary \mathbf{x} vector and a Hermitian positive definite matrix $\boldsymbol{\Sigma} > 0$ is defined as: $\|\mathbf{x}\|_{\boldsymbol{\Sigma}}^2 = \mathbf{x}^* \boldsymbol{\Sigma} \mathbf{x}$. Also, we have $\tilde{\boldsymbol{\psi}}_{k-1}^{(i)} = \mathbf{w}^o - \boldsymbol{\psi}_{k-1}^{(i)}$. The procedure for performance evaluation

is to write the energy conservation relation [4] and then proceed to find the error values. For this reason we first introduce the following quantities:

$$\begin{aligned}
\boldsymbol{\psi}^i &\triangleq \text{col}\{\boldsymbol{\psi}_1^{(i)}, \dots, \boldsymbol{\psi}_N^{(i)}\} & \mathbf{U}_i &\triangleq \text{diag}\{\mathbf{u}_{1,i}, \dots, \mathbf{u}_{N,i}\} \\
\boldsymbol{\phi}^i &\triangleq \text{col}\{\boldsymbol{\phi}_1^{(i)}, \dots, \boldsymbol{\phi}_N^{(i)}\} & \mathbf{d}_i &\triangleq \text{col}\{d_1(i), \dots, d_N(i)\} \\
\mathbf{v}_i &\triangleq \text{col}\{v_1(i), \dots, v_N(i)\} & \mathbf{w}^{(o)} &\triangleq \text{col}\{\mathbf{w}^o, \dots, \mathbf{w}^o\} \\
\mathbf{D} &\triangleq \text{diag}\{\mu_1 \mathbf{I}_M, \dots, \mu_N \mathbf{I}_M\} & \mathbf{q}^i &\triangleq \text{col}\{\mathbf{q}_1^{(i)}, \dots, \mathbf{q}_N^{(i)}\}
\end{aligned} \tag{13}$$

Since all $\mathbf{q}_{k,l}^{(i)}$ s are independent of each other, then:

$$\mathbf{Q} \triangleq \mathbb{E}[\mathbf{q}^i (\mathbf{q}^i)^*] = \text{diag}\{\mathbf{Q}_1, \dots, \mathbf{Q}_N\} \tag{14}$$

Using the linear observation model $d_k(i) = \mathbf{u}_{k,i} \mathbf{w}^o + v_k(i)$ and the definitions in (1) we have:

$$\mathbf{d}_i = \mathbf{U}_i \mathbf{w}^{(o)} + \mathbf{v}_i \tag{15}$$

Now we can write the CTA algorithm in the state space form:

$$\begin{aligned}
\boldsymbol{\phi}^{i-1} &= \mathbf{G}_i \boldsymbol{\psi}^{i-1} + \mathbf{q}^{i-1} \\
\boldsymbol{\psi}^i &= \boldsymbol{\phi}^{i-1} + \mathbf{D} \mathbf{U}_i^* (\mathbf{d}_i - \mathbf{U}_i \boldsymbol{\phi}^{i-1})
\end{aligned} \tag{16}$$

where \mathbf{G}_i is the irradiance coefficient matrix and:

$$\mathbf{G}_i = \begin{bmatrix} c_{11} & I_{12}(i)c_{12} & \dots & I_{1N}c_{1N} \\ \vdots & c_{22} & \dots & \vdots \\ \vdots & \vdots & \dots & \vdots \\ I_{N1}(i)c_{N1} & \dots & \dots & c_{NN} \end{bmatrix} \tag{17}$$

This is where we incorporate the channel irradiance coefficient values to our theoretical analysis.

The relation (16) can be written as:

$$\boldsymbol{\psi}^i = \mathbf{G}_i \boldsymbol{\psi}^{i-1} + \mathbf{q}^{i-1} + \mathbf{D} \mathbf{U}_i^* (\mathbf{d}_i - \mathbf{U}_i \mathbf{G}_i \boldsymbol{\psi}^{i-1} - \mathbf{U}_i \mathbf{q}^{i-1}) \tag{18}$$

with the subtraction of $\mathbf{w}^{(o)}$ from both sides of this equation we get [20]:

$$\begin{aligned}
\tilde{\boldsymbol{\psi}}^i &= \mathbf{G}_i \tilde{\boldsymbol{\psi}}^{i-1} + (\mathbf{I} - \mathbf{G}_i) \mathbf{w}^{(o)} - \mathbf{q}^{i-1} - \mathbf{D} \mathbf{U}_i^* (\mathbf{U}_i \mathbf{w}^{(o)} + \mathbf{v}_i - \mathbf{U}_i \mathbf{G}_i \tilde{\boldsymbol{\psi}}^{i-1} - \mathbf{U}_i \mathbf{q}^{i-1}) \\
&= \mathbf{G}_i \tilde{\boldsymbol{\psi}}^{i-1} + (\mathbf{I} - \mathbf{G}_i) \mathbf{w}^{(o)} - \mathbf{D} \mathbf{U}_i^* \mathbf{U}_i \mathbf{G}_i \tilde{\boldsymbol{\psi}}^{i-1} - \mathbf{D} \mathbf{U}_i^* \mathbf{v}_i - \mathbf{D} \mathbf{U}_i^* \mathbf{U}_i (\mathbf{I} - \mathbf{G}_i) \mathbf{w}^{(o)} - \mathbf{q}^{i-1} + \mathbf{D} \mathbf{U}_i^* \mathbf{U}_i \mathbf{q}^{i-1}
\end{aligned} \tag{19}$$

If we apply the weighted norm and expectation operators to this relation we get:

$$\mathbb{E}[\|\tilde{\boldsymbol{\psi}}^i\|_{\boldsymbol{\Sigma}}^2] = \mathbb{E}[\|\tilde{\boldsymbol{\psi}}^{i-1}\|_{\boldsymbol{\Sigma}'}^2] + \mathbb{E}[\mathbf{v}_i^* \mathbf{U}_i \mathbf{D} \boldsymbol{\Sigma} \mathbf{D} \mathbf{U}_i^* \mathbf{v}_i] + \mathbb{E}[\|\mathbf{q}^{i-1}\|_{\mathbf{H}}^2] + \|\mathbf{w}^{(o)}\|_{\mathbf{K}+\mathbf{L}}^2 \tag{20}$$

where $\mathbb{E}[\tilde{\boldsymbol{\psi}}^{i-1}] = \boldsymbol{\mathfrak{B}} \mathbf{w}^{(o)}$ and $\boldsymbol{\mathfrak{B}}$ is a matrix. Therefore [20]:

$$\begin{aligned}
\mathbf{H} &= \boldsymbol{\Sigma} - \mathbb{E}[\mathbf{U}_i^* \mathbf{U}_i] \mathbf{D} \boldsymbol{\Sigma} - \boldsymbol{\Sigma} \mathbf{D} \mathbb{E}[\mathbf{U}_i^* \mathbf{U}_i] + \mathbb{E}[\mathbf{U}_i^* \mathbf{U}_i \mathbf{D} \boldsymbol{\Sigma} \mathbf{D} \mathbf{U}_i^* \mathbf{U}_i] \\
\boldsymbol{\Sigma}' &= \mathbb{E}[\mathbf{G}_i^* \mathbf{H} \mathbf{G}_i] \\
\mathbf{K} &= \mathbb{E}[(\mathbf{I} - \mathbf{G}_i)^* \mathbf{H} (\mathbf{I} - \mathbf{G}_i)] \\
\mathbf{L} &= \mathbb{E}[\boldsymbol{\mathfrak{B}}^* \mathbf{G}_i^* \mathbf{H} (\mathbf{I} - \mathbf{G}_i)] + \mathbb{E}[(\mathbf{I} - \mathbf{G}_i) \mathbf{H} \mathbf{G}_i \boldsymbol{\mathfrak{B}}]
\end{aligned} \tag{21}$$

In order to calculate the EMSE and MSD values, we assume that the regression vectors follow a zero-mean Gaussian distribution with covariance matrix $\mathbf{R}_u = \mathbb{E}[\mathbf{U}_i^* \mathbf{U}_i] = \boldsymbol{\Lambda} \boldsymbol{\Lambda}^*$ with $\boldsymbol{\Lambda} = \text{diag}\{\boldsymbol{\Lambda}_1, \dots, \boldsymbol{\Lambda}_N\}$ as a diagonal matrix containing the eigenvalues of the covariance matrix of each node

$\mathbf{R}_{u,k} = \mathbf{T}_k \mathbf{\Lambda}_k \mathbf{T}_k^*$ where $\mathbf{T} = \text{diag}\{\mathbf{T}_1, \dots, \mathbf{T}_N\}$ and $\mathbf{T}\mathbf{T}^* = \mathbf{T}^*\mathbf{T} = \mathbf{I}$. With this assumption, we define the following quantities [20]:

$$\begin{aligned} \bar{\boldsymbol{\psi}}^i &= \mathbf{T}^* \boldsymbol{\psi}^i, & \bar{\mathbf{U}}_i &= \mathbf{U}_i \mathbf{T}, & \bar{\boldsymbol{\Sigma}} &= \mathbf{T}^* \boldsymbol{\Sigma} \mathbf{T} \\ \bar{\mathbf{H}} &= \mathbf{T}^* \mathbf{H} \mathbf{T}, & \bar{\mathbf{G}}_i &= \mathbf{T}^* \mathbf{G}_i \mathbf{T}, & \bar{\mathbf{q}}^{i-1} &= \mathbf{T}^* \mathbf{q}^{i-1} \\ \bar{\mathbf{Q}} &= \mathbf{T}^* \mathbf{Q} \mathbf{T}, & \bar{\mathbf{K}} &= \mathbf{T}^* \mathbf{K} \mathbf{T}, & \bar{\mathbf{D}} &= \mathbf{T}^* \mathbf{D} \mathbf{T} = \mathbf{D} \\ \bar{\mathbf{L}} &= \mathbf{T}^* \mathbf{L} \mathbf{T}, & \bar{\mathbf{w}}^{(o)} &= \mathbf{T}^* \mathbf{w}^{(o)}, & \bar{\boldsymbol{\mathfrak{B}}} &= \mathbf{T}^* \boldsymbol{\mathfrak{B}} \mathbf{T} = \boldsymbol{\mathfrak{B}}_i \end{aligned} \quad (22)$$

Using these definitions the equations (20) and (21) become:

$$E \left[\|\bar{\boldsymbol{\psi}}^i\|_{\bar{\boldsymbol{\Sigma}}}^2 \right] = E \left[\|\bar{\boldsymbol{\psi}}^{i-1}\|_{\bar{\boldsymbol{\Sigma}}}^2 \right] + E[\mathbf{v}_i^* \bar{\mathbf{U}}_i \mathbf{D} \bar{\boldsymbol{\Sigma}} \mathbf{D} \bar{\mathbf{U}}_i^* \mathbf{v}_i] + E \left[\|\bar{\mathbf{q}}^{i-1}\|_{\bar{\mathbf{H}}}^2 \right] + \|\bar{\mathbf{w}}^{(o)}\|_{\bar{\mathbf{K}}+\bar{\mathbf{L}}}^2 \quad (23)$$

and we have [20]:

$$\begin{aligned} \bar{\mathbf{H}} &= \bar{\boldsymbol{\Sigma}} - E[\bar{\mathbf{U}}_i^* \bar{\mathbf{U}}_i] \mathbf{D} \bar{\boldsymbol{\Sigma}} - \bar{\boldsymbol{\Sigma}} \mathbf{D} E[\bar{\mathbf{U}}_i^* \bar{\mathbf{U}}_i] + E[\bar{\mathbf{U}}_i^* \bar{\mathbf{U}}_i \mathbf{D} \bar{\boldsymbol{\Sigma}} \mathbf{D} \bar{\mathbf{U}}_i^* \bar{\mathbf{U}}_i] \\ \bar{\boldsymbol{\Sigma}}' &= E[\bar{\mathbf{G}}_i^* \bar{\mathbf{H}} \bar{\mathbf{G}}_i] \\ \bar{\mathbf{K}} &= E[(\mathbf{I} - \bar{\mathbf{G}}_i)^* \bar{\mathbf{H}} (\mathbf{I} - \bar{\mathbf{G}}_i)] \\ \bar{\mathbf{L}} &= E[\boldsymbol{\mathfrak{B}}^* \bar{\mathbf{G}}_i^* \bar{\mathbf{H}} (\mathbf{I} - \bar{\mathbf{G}}_i)] + E[(\mathbf{I} - \bar{\mathbf{G}}_i) \bar{\mathbf{H}} \bar{\mathbf{G}}_i \boldsymbol{\mathfrak{B}}] \end{aligned} \quad (24)$$

Since the moments in (23) and (24) have block-type and diagonal structures, we must use the $\text{bvec}\{\cdot\}$ operator and Kronecker products for them. Also, the following features are useful for steady-state analysis:

For each matrix \mathbf{A} , $\boldsymbol{\Sigma}$, and \mathbf{B} with the proper sizes we have:

$$\text{bvec}\{\mathbf{A}\boldsymbol{\Sigma}\mathbf{B}\} = (\mathbf{B}^T \odot \mathbf{A}) \text{bvec}\{\boldsymbol{\Sigma}\} \quad (25)$$

$$\text{Tr}(\mathbf{A}\boldsymbol{\Sigma}) = \text{bvec}\{\mathbf{A}^T\} \text{bvec}\{\boldsymbol{\Sigma}\} \quad (26)$$

with use of $\bar{\boldsymbol{\sigma}} = \text{bvec}\{\bar{\boldsymbol{\Sigma}}\}$, $E[\bar{\mathbf{U}}_i^* \bar{\mathbf{U}}_i] = \boldsymbol{\Lambda}$ and $E[\bar{\mathbf{G}}_i] = \bar{\boldsymbol{\mathcal{G}}}$ we get:

$$\text{bvec}\{\bar{\boldsymbol{\mathcal{G}}}^* \bar{\boldsymbol{\Sigma}} \bar{\boldsymbol{\mathcal{G}}}\} = (\bar{\boldsymbol{\mathcal{G}}}^T \odot \bar{\boldsymbol{\mathcal{G}}}^*) \bar{\boldsymbol{\sigma}} \quad (27)$$

$$\text{bvec}\{\bar{\boldsymbol{\mathcal{G}}}^* \bar{\boldsymbol{\Sigma}} \mathbf{D} \boldsymbol{\Lambda} \bar{\boldsymbol{\mathcal{G}}}\} = (\bar{\boldsymbol{\mathcal{G}}}^T \odot \bar{\boldsymbol{\mathcal{G}}}^*) \text{bvec}\{\mathbf{I}_{NM} \bar{\boldsymbol{\Sigma}} \mathbf{D} \boldsymbol{\Lambda}\} = (\bar{\boldsymbol{\mathcal{G}}}^T \odot \bar{\boldsymbol{\mathcal{G}}}^*) (\boldsymbol{\Lambda} \mathbf{D} \odot \mathbf{I}_{NM}) \bar{\boldsymbol{\sigma}} \quad (28)$$

$$\text{bvec}\{\bar{\boldsymbol{\mathcal{G}}}^* \boldsymbol{\Lambda} \mathbf{D} \bar{\boldsymbol{\mathcal{G}}}\} = (\bar{\boldsymbol{\mathcal{G}}}^T \odot \bar{\boldsymbol{\mathcal{G}}}^*) (\mathbf{I}_{NM} \odot \boldsymbol{\Lambda} \mathbf{D}) \bar{\boldsymbol{\sigma}} \quad (29)$$

$$\text{bvec}\{\bar{\boldsymbol{\mathcal{G}}}^* \bar{\mathbf{U}}_i^* \bar{\mathbf{U}}_i \mathbf{D} \bar{\boldsymbol{\Sigma}} \mathbf{D} \bar{\mathbf{U}}_i^* \bar{\mathbf{U}}_i \bar{\boldsymbol{\mathcal{G}}}\} = (\bar{\boldsymbol{\mathcal{G}}}^T \odot \bar{\boldsymbol{\mathcal{G}}}^*) (\mathbf{D} \odot \mathbf{D}) \text{bvec}\{\mathbf{A}\} \quad (30)$$

In equation (30), $\mathbf{A} \triangleq E[\bar{\mathbf{U}}_i^* \bar{\mathbf{U}}_i \bar{\boldsymbol{\Sigma}} \mathbf{D} \bar{\mathbf{U}}_i^* \bar{\mathbf{U}}_i]$ and $\mathbf{A} = [\mathbf{A}_{kl}]$ is a block matrix. In order to calculate $\text{bvec}\{\mathbf{A}\}$, all the blocks of this matrix must be calculated. For the kl th block of this matrix we have:

$$\mathbf{A}_{kl} = E[\bar{\mathbf{U}}_{k,i}^* \bar{\mathbf{U}}_{k,i} \bar{\boldsymbol{\Sigma}}_{kl} \bar{\mathbf{U}}_{l,i}^* \bar{\mathbf{U}}_{l,i}] = \begin{cases} \boldsymbol{\Lambda}_k \text{Tr}(\boldsymbol{\Lambda}_k \bar{\boldsymbol{\Sigma}}_{kk}) + \gamma \boldsymbol{\Lambda}_k \bar{\boldsymbol{\Sigma}}_{kk} \boldsymbol{\Lambda}_k & k = l \\ \boldsymbol{\Lambda}_k \bar{\boldsymbol{\Sigma}}_{kl} \boldsymbol{\Lambda}_l & k \neq l \end{cases} \quad (31)$$

and for $\text{vec}\{\mathbf{A}_{kl}\}$:

$$\mathbf{a}_{kl} = \text{vec}\{\mathbf{A}_{kl}\} = \begin{cases} (\boldsymbol{\Lambda}_k \boldsymbol{\Lambda}_k^T + \gamma \boldsymbol{\Lambda}_k \otimes \boldsymbol{\Lambda}_k) \bar{\boldsymbol{\sigma}}_{kk} & k = l \\ (\boldsymbol{\Lambda}_k \otimes \boldsymbol{\Lambda}_l) \bar{\boldsymbol{\sigma}}_{kl} & k \neq l \end{cases} \quad (32)$$

then we collect all the \mathbf{a}_{kl} values in a vector:

$$\mathbf{a}_l = [\mathbf{a}_{1l}, \mathbf{a}_{2l}, \dots, \mathbf{a}_{kl}, \dots, \mathbf{a}_{Nl}]^T \triangleq \mathcal{A}_l \bar{\boldsymbol{\sigma}}_l \quad (33)$$

where:

$$\mathcal{A}_i = \text{diag}\{\Lambda_1 \otimes \Lambda_i, \dots, +\lambda_i \lambda_i^T + \gamma \Lambda_i \otimes \Lambda_i, \dots, \Lambda_N \otimes \Lambda_i\} \quad (34)$$

Using the above equation we have:

$$\text{bvec}\{\mathbf{A}\} = \text{col}\{\mathcal{A}_1 \bar{\boldsymbol{\sigma}}_1, \mathcal{A}_2 \bar{\boldsymbol{\sigma}}_2, \dots, \mathcal{A}_N \bar{\boldsymbol{\sigma}}_N\} = \mathcal{A} \bar{\boldsymbol{\sigma}} \quad (35)$$

where $\mathcal{A} = \text{diag}\{\mathcal{A}_1, \mathcal{A}_2, \dots, \mathcal{A}_N\}$. For the rest of the needed moments we calculate:

$$\mathbb{E}[\mathbf{v}_i^* \bar{\mathbf{U}}_i \mathbf{D} \bar{\boldsymbol{\Sigma}} \mathbf{D} \bar{\mathbf{U}}_i^* \mathbf{v}_i] = \text{Tr}(\Lambda_v \mathbb{E}[\bar{\mathbf{U}}_i \mathbf{D} \bar{\boldsymbol{\Sigma}} \mathbf{D} \bar{\mathbf{U}}_i^*]) = \mathbf{b}^T \bar{\boldsymbol{\sigma}} \quad (36)$$

in this relation, we have $\mathbf{b} = \text{bvec}\{\mathbf{R}_v \mathbf{D}^2 \Lambda\}$, $\Lambda_v = \text{diag}\{\sigma_{v,1}^2, \sigma_{v,2}^2, \dots, \sigma_{v,N}^2\}$ and $\mathbf{R}_v = \Lambda_v \odot \mathbf{I}_M$. The moments relating to noisy links are [20]:

$$\mathbb{E}[(\bar{\mathbf{q}}^{i-1})^* \bar{\boldsymbol{\Sigma}} \bar{\mathbf{q}}^{i-1}] = \text{Tr}(\mathbb{E}[\bar{\mathbf{q}}^{i-1} (\bar{\mathbf{q}}^{i-1})^*] \bar{\boldsymbol{\Sigma}}) = \text{Tr}(\bar{\mathbf{Q}} \bar{\boldsymbol{\Sigma}}) = \text{bvec}\{\bar{\mathbf{Q}}^T\}^T \bar{\boldsymbol{\sigma}} \quad (37)$$

$$\mathbb{E}[(\bar{\mathbf{q}}^{i-1})^* \bar{\mathbf{U}}_i^* \bar{\mathbf{U}}_i \mathbf{D} \bar{\boldsymbol{\Sigma}} \bar{\mathbf{q}}^{i-1}] = \text{Tr}(\mathbb{E}[\bar{\mathbf{q}}^{i-1} (\bar{\mathbf{q}}^{i-1})^*] \mathbb{E}[\bar{\mathbf{U}}_i^* \bar{\mathbf{U}}_i] \mathbf{D} \bar{\boldsymbol{\Sigma}}) = \text{Tr}(\bar{\mathbf{Q}} \Lambda \mathbf{D} \bar{\boldsymbol{\Sigma}}) = \text{bvec}\{\bar{\mathbf{Q}}^T\}^T (\mathbf{I}_{NM} \odot \Lambda \mathbf{D}) \bar{\boldsymbol{\sigma}} \quad (38)$$

$$\mathbb{E}[(\bar{\mathbf{q}}^{i-1})^* \bar{\boldsymbol{\Sigma}} \mathbf{D} \bar{\mathbf{U}}_i^* \bar{\mathbf{U}}_i \bar{\mathbf{q}}^{i-1}] = \text{bvec}\{\bar{\mathbf{Q}}^T\}^T (\Lambda \mathbf{D} \odot \mathbf{I}_{NM}) \bar{\boldsymbol{\sigma}} \quad (39)$$

$$\mathbb{E}[(\bar{\mathbf{q}}^{i-1})^* \bar{\mathbf{U}}_i^* \bar{\mathbf{U}}_i \mathbf{D} \bar{\boldsymbol{\Sigma}} \mathbf{D} \bar{\mathbf{U}}_i^* \bar{\mathbf{U}}_i \bar{\mathbf{q}}^{i-1}] = \text{Tr}(\bar{\mathbf{Q}} \mathbf{E}[\bar{\mathbf{U}}_i^* \bar{\mathbf{U}}_i] \mathbf{D} \bar{\boldsymbol{\Sigma}} \mathbf{D} \bar{\mathbf{U}}_i^* \bar{\mathbf{U}}_i) = \text{bvec}\{\bar{\mathbf{Q}}^T\}^T (\mathbf{D} \odot \mathbf{D}) \mathcal{A} \bar{\boldsymbol{\sigma}} \quad (40)$$

By substituting the above moments in relations (23) and (24) and with the definition of the matrix $\mathbf{W} = \bar{\mathbf{w}}^{(o)} (\bar{\mathbf{w}}^{(o)})^* = \mathbf{w}^{(o)} (\mathbf{w}^{(o)})^*$ we get:

$$\mathbb{E}[\|\bar{\boldsymbol{\psi}}^i\|_{\bar{\boldsymbol{\sigma}}}^2] = \mathbb{E}[\|\bar{\boldsymbol{\psi}}^{i-1}\|_{\mathbf{F}\bar{\boldsymbol{\sigma}}}^2] + \mathbf{b}^T \bar{\boldsymbol{\sigma}} + \text{bvec}\{\bar{\mathbf{Q}}^T\}^T \mathbf{S} \bar{\boldsymbol{\sigma}} + \text{Tr}\{\mathbf{W}(\bar{\mathbf{K}} + \bar{\mathbf{L}})\} \quad (41)$$

and,

$$\bar{\mathbf{F}} = (\bar{\mathcal{G}}^T \odot \bar{\mathcal{G}}^*) [\mathbf{I}_{N^2 M^2} - (\mathbf{I}_{NM} \odot \Lambda \mathbf{D})] - (\Lambda \mathbf{D} \odot \mathbf{I}_{NM}) + (\mathbf{D} \odot \mathbf{D}) \mathcal{A} \quad (42)$$

Using the following relations

$$\text{bvec}\{\bar{\mathbf{K}}\} = (\mathbf{I} - \bar{\mathcal{G}})^T \odot (\mathbf{I} - \bar{\mathcal{G}})^* \mathbf{S} \bar{\boldsymbol{\sigma}} \quad (43)$$

$$\text{bvec}\{\bar{\mathbf{L}}\} = [(\mathbf{I} - \bar{\mathcal{G}})^T \odot (\bar{\mathcal{G}} \boldsymbol{\mathfrak{B}})^* + (\bar{\mathcal{G}} \boldsymbol{\mathfrak{B}})^T \odot (\mathbf{I} - \bar{\mathcal{G}})^*] \mathbf{S} \bar{\boldsymbol{\sigma}} \quad (44)$$

we have:

$$\mathbb{E}[\|\bar{\boldsymbol{\psi}}^i\|_{\bar{\boldsymbol{\sigma}}}^2] = \mathbb{E}[\|\bar{\boldsymbol{\psi}}^{i-1}\|_{\mathbf{F}\bar{\boldsymbol{\sigma}}}^2] + \mathbf{g} \bar{\boldsymbol{\sigma}} \quad (45)$$

$$\bar{\mathbf{F}} = (\bar{\mathcal{G}}^T \odot \bar{\mathcal{G}}^*) \mathbf{S} \quad (46)$$

where the \mathbf{g} and \mathbf{S} quantities are:

$$\mathbf{S} = [\mathbf{I}_{N^2 M^2} - (\mathbf{I}_{NM} \odot \Lambda \mathbf{D})] - (\Lambda \mathbf{D} \odot \mathbf{I}_{NM}) + (\mathbf{D} \odot \mathbf{D}) \mathcal{A} \quad (47)$$

$$\mathbf{g} = \mathbf{b}^T + \text{bvec}\{\bar{\mathbf{Q}}^T\}^T \mathbf{S} + \text{bvec}\{\mathbf{W}^T\}^T [(\mathbf{I} - \bar{\mathcal{G}})^T \odot (\mathbf{I} - \bar{\mathcal{G}})^* + (\mathbf{I} - \bar{\mathcal{G}})^T \odot (\bar{\mathcal{G}} \boldsymbol{\mathfrak{B}})^* + (\bar{\mathcal{G}} \boldsymbol{\mathfrak{B}})^T \odot (\mathbf{I} - \bar{\mathcal{G}})^*] \mathbf{S} \quad (48)$$

We will use (11) and (12) for achieving the steady-state behavior of diffusion LMS algorithm:

$$MSD = \frac{1}{N} \sum_{k=1}^N \eta_k = \frac{1}{N} \lim_{i \rightarrow \infty} \mathbb{E}[\|\bar{\boldsymbol{\psi}}^i\|_i^2] \quad (49)$$

$$EMSE = \frac{1}{N} \sum_{k=1}^N \zeta_k = \frac{1}{N} \lim_{i \rightarrow \infty} \mathbb{E}[\|\bar{\boldsymbol{\psi}}^i\|_{\Lambda}^2] \quad (50)$$

In the steady-state condition, we have $\mathbb{E}[\|\bar{\psi}^i\|^2] = \mathbb{E}[\|\bar{\psi}^{i-1}\|^2]$ and therefore, we can write (45) as:

$$\mathbb{E}[\|\bar{\psi}^\infty\|_{(I-\bar{F})\bar{\sigma}}^2] = \mathbf{g}\bar{\sigma} \quad i \rightarrow \infty \quad (51)$$

Now with choosing suitable values for $\bar{\sigma}$ we can achieve MSD, EMSE and MSE values. For example, by choosing it so that we have $(I - \bar{F})\bar{\sigma} = \mathbf{r}$ we get the MSD value:

$$MSD = \frac{1}{N} \mathbf{g}(I - \bar{F})^{-1} \mathbf{r} \quad (52)$$

where $\mathbf{r} = \text{bvec}\{\mathbf{I}_{NM}\}$. Likewise, by choosing $\bar{\sigma}$ so that $(I - \bar{F})\bar{\sigma} = \lambda$ we have:

$$EMSE = \frac{1}{N} \mathbf{g}(I - \bar{F})^{-1} \lambda \quad (53)$$

where $\lambda = \text{bvec}\{\mathbf{\Lambda}\}$. For each node in steady-state condition we have:

$$MSD_k = \mathbf{g}(I - \bar{F})^{-1} \text{bvec}\{\mathbf{J}_{r,k}\} \quad (54)$$

$$EMSE_k = \mathbf{g}(I - \bar{F})^{-1} \text{bvec}\{\mathbf{J}_{\lambda,k}\} \quad (55)$$

where:

$$\mathbf{J}_{r,k} = \text{diag}\{\mathbf{0}_{(k-1)M}, \mathbf{I}_M, \mathbf{0}_{(N-k)M}\} \quad (56)$$

$$\mathbf{J}_{\lambda,k} = \text{diag}\{\mathbf{0}_{(k-1)M}, \mathbf{\Lambda}_k, \mathbf{0}_{(N-k)M}\} \quad (57)$$

As we can see, the \mathbf{g} in equation (54) and (55) is directly dependent on the FSO channel coefficients. Therefore, using these relations we can evaluate the theoretical impact of the very strong turbulence on the CTA diffusion network.

IV. SIMULATION RESULTS

The aim of the diffusion adaptive network, in all conditions, is to converge to the desired weight vector \mathbf{w}^o . For our simulations, this weight vector is taken to be a 4×1 vector $\mathbf{w}^o = [1 \ 1 \ 1 \ 1]^T / \sqrt{4}$ ($M = 4$) with the entries that are randomly selected between -1 and 1. The step-size for all the simulations is taken to be 0.0045. The input data and the noise variables (both measurement noise and the link noise) are produced with the Gaussian distribution. The measurement noise is the noise that contaminates the sensor measurement task and is shown in this paper with $v_{k,i}$ with variance $\sigma_v^2 = 0.001$, however, the link noise or channel noise contaminates the local estimations that are communicated between the nodes and is shown in the paper with $q_{k,i}$ and variance $\sigma_c^2 = 0.001$. Also, the Eigen spread of the covariance matrix of the input variables ($\mathbf{R}_{u,k}$) is considered to be between 1

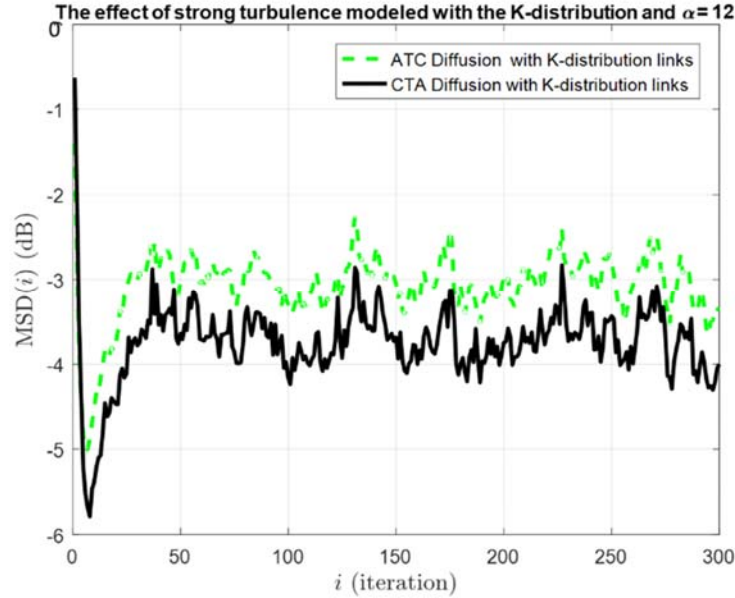


Fig. 7. Diffusion network performance in the presence of strong turbulence conditions modeled with the K-distribution

and 5. As we mentioned, the FSO link among nodes is considered to be modeled with strong turbulence or with Gaussian noise. Our network contains 20 nodes. For our first simulation, we conducted a scenario in which we could see the performance comparison of adaptive diffusion CTA and ATC networks in 3 conditions namely the ideal link condition, the noisy link condition and the strong turbulence condition modeled with the negative exponential distribution. The simulation results are produced by the computer simulations using the MATLAB software version R2016b and the theoretical results are produced by the mathematical calculations that are given through the paper. The results are presented for the node 1 in Fig. 6, and they show the very high difference between the performances in these conditions:

For the noisy and without turbulence environment, the estimation error values must be around -30 dBs. In the strong turbulence conditions however, the error values become very close to 0 dB which shows a large amount of error that is nearly useless for an adaptive network. It means that the network in a strong turbulence environment becomes very weak and in order to strengthen it, we must take countermeasure actions like channel estimation for the performance improvement.

In order to present the performance of the diffusion networks in FSO links with strong turbulence, we design two simulation cases the first simulation is designed with the assumption that the FSO links are modeled with the k-distribution. As we observed in section III, the K-distribution parameter I_0 can change the PDF and model and therefore can change directly the FSO link coefficients. Our analysis showed that the diffusion network can only converge to w^o when the α is 12. The simulation results for ATC and CTA diffusion algorithms are given in Fig. 7 with k-distribution link models.

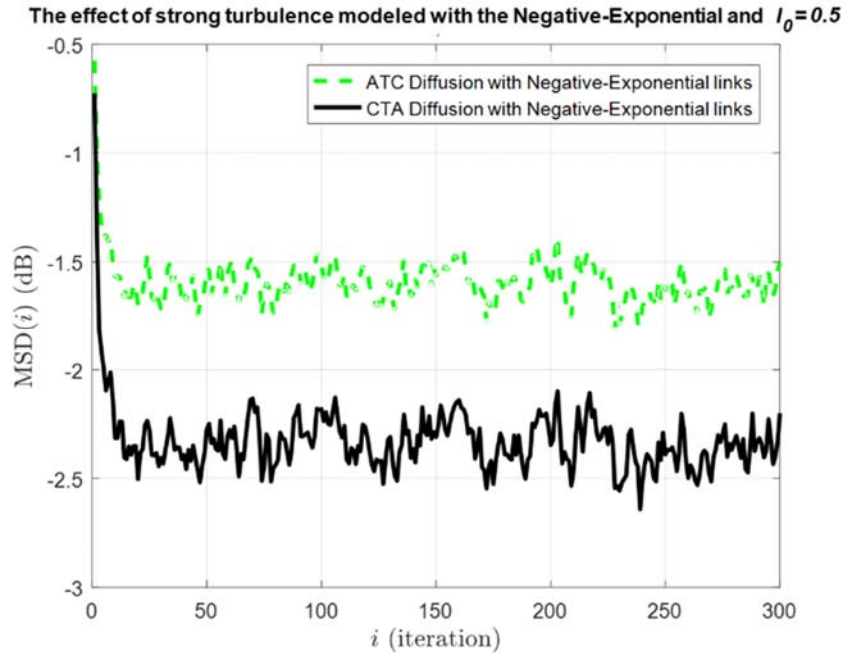


Fig. 8. Diffusion network performance in the presence of strong turbulence conditions modeled with the Negative-Exponential distribution.

In the second case, we consider the negative exponential model assumption for the FSO links. In these simulations, the I_0 parameter can determine the shape of PDF and the values or link coefficients. Likewise, our analysis showed that the only I_0 value that the diffusion network can tolerate is $I_0 = 0.5$ and in this case, even the performance is not very good. The results are shown in Fig. 8 confirm the network need for channel estimation.

Here, using the equation (54) we present and compare the theoretical and simulation results of the CTA diffusion strategy in both Negative exponential and K-distribution conditions. As we can see, there is a very close match between the simulation and theoretical findings of the diffusion network performance in the very strong FSO turbulence conditions.

V. CONCLUSIONS

Adaptive networks can be implemented in different link conditions using various technologies. The important thing is how well they work in these cases. In order to investigate this, we must perform various simulations depending on the exact distributions of the link models. We investigated the performance of the diffusion CTA and ATC networks with FSO links that were suffering from strong turbulence conditions. For this reason, we considered the link models to follow a negative exponential and k-distribution. The results showed very poor performances for these conditions and therefore, entail the need for usage of channel estimation for better performances. In future works, we will

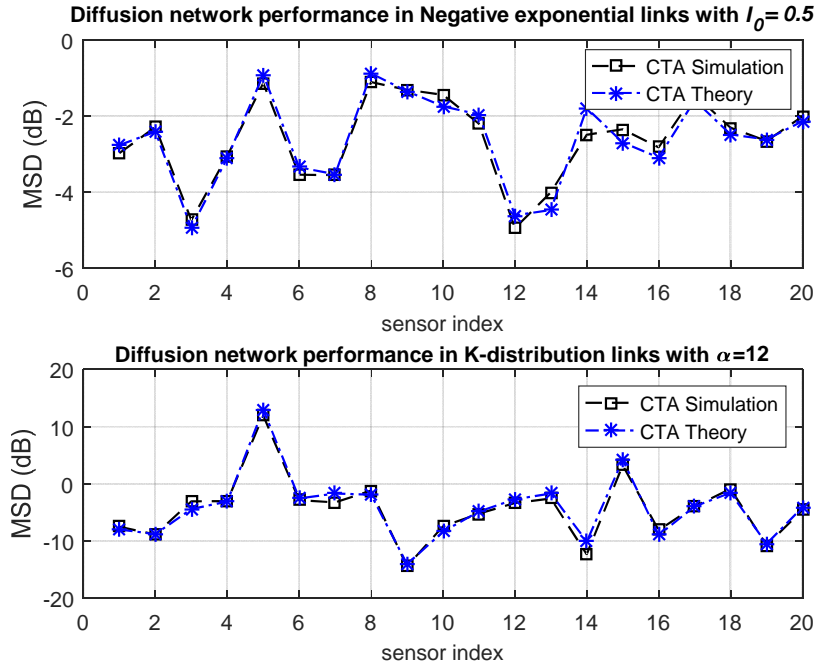


Fig. 9. The theoretical performance of the Diffusion network with CTA strategy in the presence of strong turbulence conditions modeled with the Negative-Exponential and K-distributions.

pursue the channel estimation for FSO communication systems with adaptive networks. Also, we will analyze the performance of the diffusion networks in other FSO channel models.

REFERENCES

- [1] Z. Ghassemlooy, W. Popoola, and S. Rajbhandari, *Visible light communications theory and applications*, CRC Press, NY, 2017.
- [2] X. Zhu and J. M. Kahn, "Free-space optical communication through atmospheric turbulence channels," *IEEE Trans. Commun.*, vol. 50, no. 8, pp. 1293-1300, Aug. 2002.
- [3] Z. Ghassemlooy, W. Popoola, and S. Rajbhandari, *Optical wireless communications system and channel modeling with MATLAB*, CRC Press, NY, 2013.
- [4] N. Mishra, D. Sriram Kumar, "Outage analysis of relay-assisted FSO systems over K-distribution turbulence channel," *International Conference on Electrical, Electronics, and Optimization Techniques (ICE OT)*, 3-5 March 2016.
- [5] I. K. Son, S. Mao, *A Survey of Free Space Optical Networks, Digital Communications, and Networks*, vol. 3, no. 2, pp. 67-77, 2017.
- [6] H.E. Nistazakisa, V.D. Assimakopoulosb, and G.S. Tombrasa, "Performance estimation of free space optical links over negative exponential atmospheric turbulence channels," *Optik*, vol. 122, no. 24, pp. 2191-2194, Dec. 2011.
- [7] M. Uysal, L. Jing, and Y. Meng, "Error rate performance analysis of coded free-space optical links over Gamma-Gamma atmospheric turbulence channels," *IEEE Trans. Wireless Commun.*, vol. 5, no. 6, pp. 1229-1233, June 2006.
- [8] T.A. Tsiftsis, H.G. Sandalidis, G.K. Karagiannidis, and M. Uysal, "Optical wireless links with spatial diversity over strong atmospheric turbulence channels," *IEEE Transactions on Wireless Communications*, vol. 8, no. 2, pp. 951-957, Feb. 2009.

- [9] M. Uysal, S. Mohammad Navidpour, and Jing Li. "Error rate performance of coded free-space optical links over strong turbulence channels," *IEEE Communications Letters*, vol. 8, no. 10, pp. 635-637, Oct. 2004.
- [10] N. Mingbo, J. Cheng, J. F. Holzman, and L. McPhail. "Performance analysis of coherent free-space optical communication systems with K-distributed turbulence," *IEEE International Conference on Communications*, pp. 1-5, 2009.
- [11] M. Uysal, C. Capsoni, Z. Ghassemlooy, W. Popoola, and S. Rajbhandari, *Optical wireless communications*, Springer International Publishing Switzerland, 2016.
- [12] W. O. Popoola, Z. Ghassemlooy, A. Boucouvalac, and E. Udvary, "Free-space optical communication using subcarrier modulation in gamma-gamma atmospheric turbulence," *Proc. 9th ICTON*, Rome, Italy, vol. 3, pp. 156-160, 2007.
- [13] A. Khalili, M.A. Tinati, A. Rastegarnia, and J.A. Chambers, "Steady state analysis of diffusion LMS adaptive networks with noisy links," *IEEE Transactions on Signal Process.* vol. 60, no. 2, pp. 974-979, Feb. 2012.
- [14] R. Abdolee, B. Champagne, and A. H. Sayed, "Diffusion LMS strategies for parameter estimation over fading wireless channels," *IEEE international conference on communications*, pp. 1926-1930, 2013.
- [15] A. Aminfar, Ch. Ghobadi, and M. Chehel Amirani, "Diffusion adaptation through free space optical (FSO) wireless communication channels," *IEEE 4th International Conference on Knowledge-Based Engineering and Innovation (KBEI-2017)*, Dec. 22nd, Tehran, Iran, 2017.
- [16] E. Mostafapour, Ch. Ghobadi, J. Nourinia, and M. Chehel Amirani, "Tracking performance of incremental LMS algorithm over adaptive distributed sensor network," *Journal of communication engineering*, vol. 4, no. 1, pp. 55-66, Winter-Spring 2015.
- [17] E. Mostafapour, Ch.Ghobadi, and M.C. Amirani, "Non-stationary channel estimation with diffusion adaptation strategies over distributed networks," *Wireless Personal Communication*, vol. 99, no. 3, pp. 1377-1390, April 2018.
- [18] A. Khalili, A. Rastegarnia, and S. Sanei, "Performance analysis of incremental LMS over flat fading channels," *IEEE Trans. control of network systems*, vol. 4, no. 3, pp. 489-498, Sept. 2017.
- [19] M. A. Al-Habash, L. C. Andrews, and R. L. Phillips, "Mathematical model for the irradiance probability density function of a laser beam propagating through turbulent media," *Optical Engineering.*, vol. 40, no. 8, pp. 1554-1562, Aug. 2001.
- [20] A. Khalili, A. Rastegarnia, V. Vahidpour, and TY. Rezaei, "On the Effects of Flat Fading Channels on the Steady-State Performance of Diffusion Adaptive Networks," *Journal of advanced signal processing*, vol. 1, no. 1, pp. 27-34, 2016.
- [21] E. Mostafapour, et al., "The Implementation of Adaptive Networks with Visible Light Communication Channels Modeled with Gamma-Gamma Turbulence," *2nd West Asian Colloquium on Optical Wireless Communications (WACOWC)*, Tehran, Iran, 27-28 April, 2019.